Supporting Information for *'Relative rate of change in cognitive score network dynamics via Bayesian hierarchical model reveal spatial patterns of neurodegeneration'*

April 27, 2020

S.1 Exploratory analyses on cortical thickness response

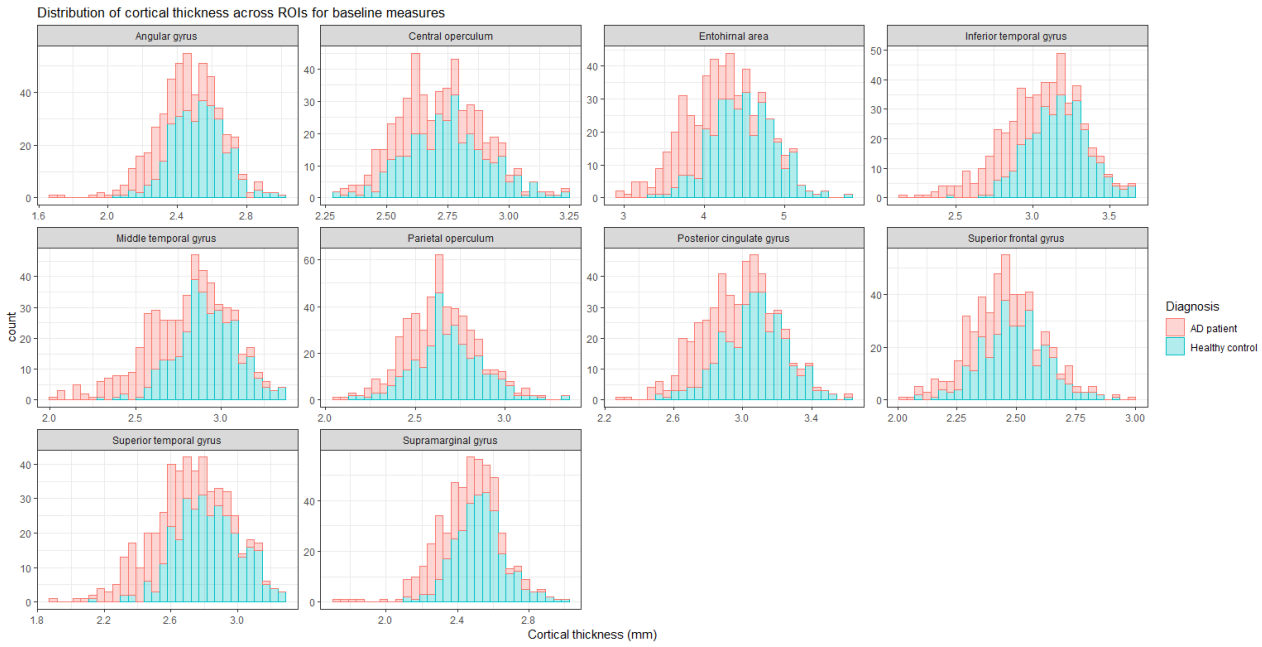

Figure 1: Histogram of ten cortical thickness regions at baseline for healthy control participants (blue) and Alzheimer disease patients (red).

S.2 Prior specification and parameter estimation

S.2.1 Prior and conditional distributions for σ^2, σ_s^2 and β

Inverse gamma distributions were chosen for the spatial scale σ_s^2 and residual σ^2 variance terms, which led to conditionally-conjugate [3] priors whose full conditional distributions are of the following forms

$$p(\sigma_s^2|W,\mathbf{b}) \sim IG\left(\frac{IK+2c}{2}, \frac{1}{2}\sum_{i=1}^{I}\mathbf{b}_i Q_i^{-1}\mathbf{b}_i + d\right), \tag{1}$$

and

$$p(\sigma^2|\mathbf{b},\boldsymbol{\beta},X) \sim IG\left(\frac{N+2e}{2}, \frac{1}{2}\left(\sum_{i=1}^{I}\sum_{r=1}^{R_i}\sum_{k=1}^{K}(y_{irk}-\mathbf{x}_i\boldsymbol{\beta}-b_{ik})^2\right)+f\right), \tag{2}$$

where the hyperparameter for these priors are $IG(c,d)$ and $IG(e,f)$ for the spatial scale and residual terms respectively, and N is the total number of observations.

In keeping with Lu et al [4] and Cespedes et al, [1] the fixed effect parameter $\boldsymbol{\beta}$ has a multivariate normal distribution $MVN(\boldsymbol{\mu}_0, \Sigma_0)$ prior, with hyperparameters chosen such that the prior is relatively uninformative for the range of cortical thickness values expected to be observed. The full conditional distribution for $\boldsymbol{\beta}$ is

$$p(\boldsymbol{\beta}|\mathbf{b},\mathbf{y},X,\sigma^2) \sim MVN\left(\left[\frac{1}{\sigma^2}\overset{L}{X}^T\overset{L}{X}+\Sigma_0^{-1}\right]^{-1}\left[\frac{1}{\sigma^2}\overset{L}{X}^T(\overset{\mathbf{L}}{\mathbf{y}}-\overset{\mathbf{L}}{\mathbf{b}})+\Sigma_0^{-1}\boldsymbol{\mu}_0\right], \left[\frac{1}{\sigma^2}\overset{L}{X}^T\overset{L}{X}+\Sigma_0^{-1}\right]^{-1}\right), \tag{3}$$

where the long vector form of the response $\mathbf{y}$, spatial random effects $\mathbf{b}$ and covariance matrix X are $\overset{L}{\mathbf{y}}$, $\overset{L}{\mathbf{b}}$ and $\overset{L}{X}$ respectively.

S.2.2 Posterior draws for spatial random effects $\mathbf{b}_i$

The full conditional distribution of $\mathbf{b}_i$ is given by

$$p(\mathbf{b}_i|\boldsymbol{\beta},\sigma^2,W^i,\sigma_s^2,X,\mathbf{y}) \sim MVN\left(\left[\frac{1}{\sigma_s^2}Q_i^{-1}+\frac{R_i}{\sigma^2}\mathbb{1}\right]^{-1}\left[\frac{1}{\sigma^2}\left(\sum_{r=1}^{R_i}\mathbf{y}_{ir}-(\mathbf{x}_i\boldsymbol{\beta})\mathbf{e}\right)\right], \left[\frac{1}{\sigma_s^2}Q_i^{-1}+\frac{R_i}{\sigma^2}\mathbb{1}\right]^{-1}\right), \tag{4}$$

where the unit vector $\mathbf{e} = [1,1,...,1]$ is of length K.

S.2.3 Posterior sampling for brain connectivity matrix W^i with respect to cognitive score

Draws from W^i are updated element-wise at each annual relative rate of change of cognitive score of participant i. A connection between region m and n for CS_i of person i is w_{mn}^i, and as shown in Figure 1 and Model (1), w_{mn}^i is equated to zero or one according to a Bernoulli distribution with probability p_{mn}^i.

It follows from the posterior distribution in (3) that the full conditional distribution for w_{mn}^i is

$$p(w_{mn}^i|\sigma_s^2,\mathbf{b}_i,\gamma_{mn}^0,\gamma_{mn}^1,W^i,CS_i) \propto p(\mathbf{b}_i|\sigma_s^2,W^i)p(w_{mn}^i|\gamma_{mn}^0,\gamma_{mn}^1,CS_i).$$

The log-transformation of the expression above is

$$\log[p(w_{mn}^i|.)] \propto \frac{1}{2}\log|Q_i^{-1}| - \frac{1}{2\sigma_s^2}\mathbf{b}_i Q_i^{-1}\mathbf{b}_i + w_{mn}^i(\gamma_{mn}^0+\gamma_{mn}^1 CS_i) - \log(1+\exp(\gamma_{mn}^0+\gamma_{mn}^1 CS_i)),$$

up to an additive constant. This log-expression is evaluated at $w_{mn}^i = 1$ and 0, resulting with expressions for $\log p_1$ and $\log p_0$ respectively. The probability of $p(w_{mn}^i = 1)$ taking into account the normalising constant is

$$p_1^* = \frac{p_1}{p_1 + p_0} = \frac{1}{1 + \exp(\log p_0 - \log p_1)}.$$

For numerical reasons, since p_0 and p_1 are generally very small, we work with the expression on the right. Draws w_{mn}^{i*} are updated by $w_{mn}^{i*} \sim Bern(p_1^*)$.

S.2.4 Adaptive Metropolis Hastings scheme for $\boldsymbol{\gamma}_{mn}$

The matrix γ^1 indicates the change in the log-odds of a link between nodes for each unit increase in annual relative rate of change in cognitive score (CS_i). If the credible intervals for the elements of γ^1 exclude zero, then CS_i is inferred to play an important role in explaining the network architecture. Consequently inferences can be made about whether connections observed in the network appear or disappear with respect to CS_i.

Draws for parameters γ_{mn}^0 and γ_{mn}^1 are updated simultaneously through the vector $\boldsymbol{\gamma}_{mn} = [\gamma_{mn}^0, \gamma_{mn}^1]$, via a multivariate normal random walk MH step, [2, 5] as the full conditional distributions are not of a known closed form. The priors for $p(\boldsymbol{\gamma}_{mn})$ are multivariate normal with mean $\boldsymbol{\mu}_\gamma$ and diagonal covariance matrix Σ_γ. Diagonal elements of Σ_γ were set to 5 so that the probability p_{mn}^i remains relatively uninformative on the logit scale.

It follows from the posterior distribution in Expression (3) that the full conditional distribution for $\boldsymbol{\gamma}_{mn}$ is of the form

$$p(\boldsymbol{\gamma}_{mn}|w_{mn}^i, CS) \propto \prod_{i=1}^{I} \left[\frac{\exp(\gamma_{mn}^0 + \gamma_{mn}^1 CS_i)}{1 + \exp(\gamma_{mn}^0 + \gamma_{mn}^1 CS_i)}\right]^{w_{mn}^i} \left[\frac{\exp(\gamma_{mn}^0 + \gamma_{mn}^1 CS_i)}{1 + \exp(\gamma_{mn}^0 + \gamma_{mn}^1 CS_i)}\right]^{1-w_{mn}^i}$$
$$|\Sigma_\gamma|^{-1/2} \exp\left\{-\frac{1}{2}(\boldsymbol{\gamma}_{mn} - \boldsymbol{\mu}_\gamma)^T \Sigma_\gamma^{-1} (\boldsymbol{\gamma}_{mn} - \boldsymbol{\mu}_\gamma)\right\}. \quad (5)$$

The values of γ^0 and γ^1 were jointly updated by drawing independent proposals, $\boldsymbol{\gamma}_{mn}^*$, from a multivariate normal random walk and accepting the proposals with probability

$$\alpha = \min\left\{1, \frac{p(\boldsymbol{\gamma}_{mn}^*|w_{mn}, CS)}{p(\boldsymbol{\gamma}_{mn}|w_{mn}, CS)}\right\}.$$

The random walk proposals were adapted such that the acceptance rates after 100 MCMC iterations would either converge to or remain between 0.2 and 0.4.

S.3 Simulation study

A thorough assessment of the dynamic wombling model was performed via a simulation study described in Section 3 of the manuscript. One hundred independent simulated data sets were generated and the dynamic wombling algorithm was applied to each to assess the recovery of the values used to simulated the data. Table 1 shows the recovered proportion for parameters β_0, β_1 and σ^2. Section 3 discussed the expected biased estimates of σ_s^2 and the implications with respect to the other parameters, particularly W. For this reason results for σ_s^2 are not reported.

Each vertical line in the plots in Figure 2 represents a simulation run, where the point in each line is the posterior mean and its length denotes the 95% credible intervals. The underlying solution we wish to recover for each parameter is shown by the red horizontal line. The parameter estimation on a single simulation run is said to have recovered the solution, if the solution is within the credible intervals. Figure 2 shows the range of simulation solutions for parameters β_0, β_1 and σ^2 for all 100 simulated data sets. We see that in general, out of 100 simulations, based on 95% credible intervals, we recovered the solution approximately 95% of the time.

Table 1: Proportion of fixed effect (β_0 and β_1) and residual variance (σ^2) parameters recovered for the unbalanced simulation scenario, repeated 100 times.

	Proportion of recovery
β_0	95
β_1	92
σ^2	98

There are 200 participants in each simulated data set each with 10 spatial observations; this implies there are 2,000 random effects in total to recover in one application of dynamic wombling on a single data set. As there are 100 independent replicates for the simulated study, this means there are 200,000 random effects to assess if the true value lies inside the 95% credible interval. The results on the recovery of the random effects are visualised in a histogram shown in Figure 3. A large number of random effects were recovered 95% of the time which suggests the dynamic wombling algorithm adequately modelled the random effects in our simulated data.

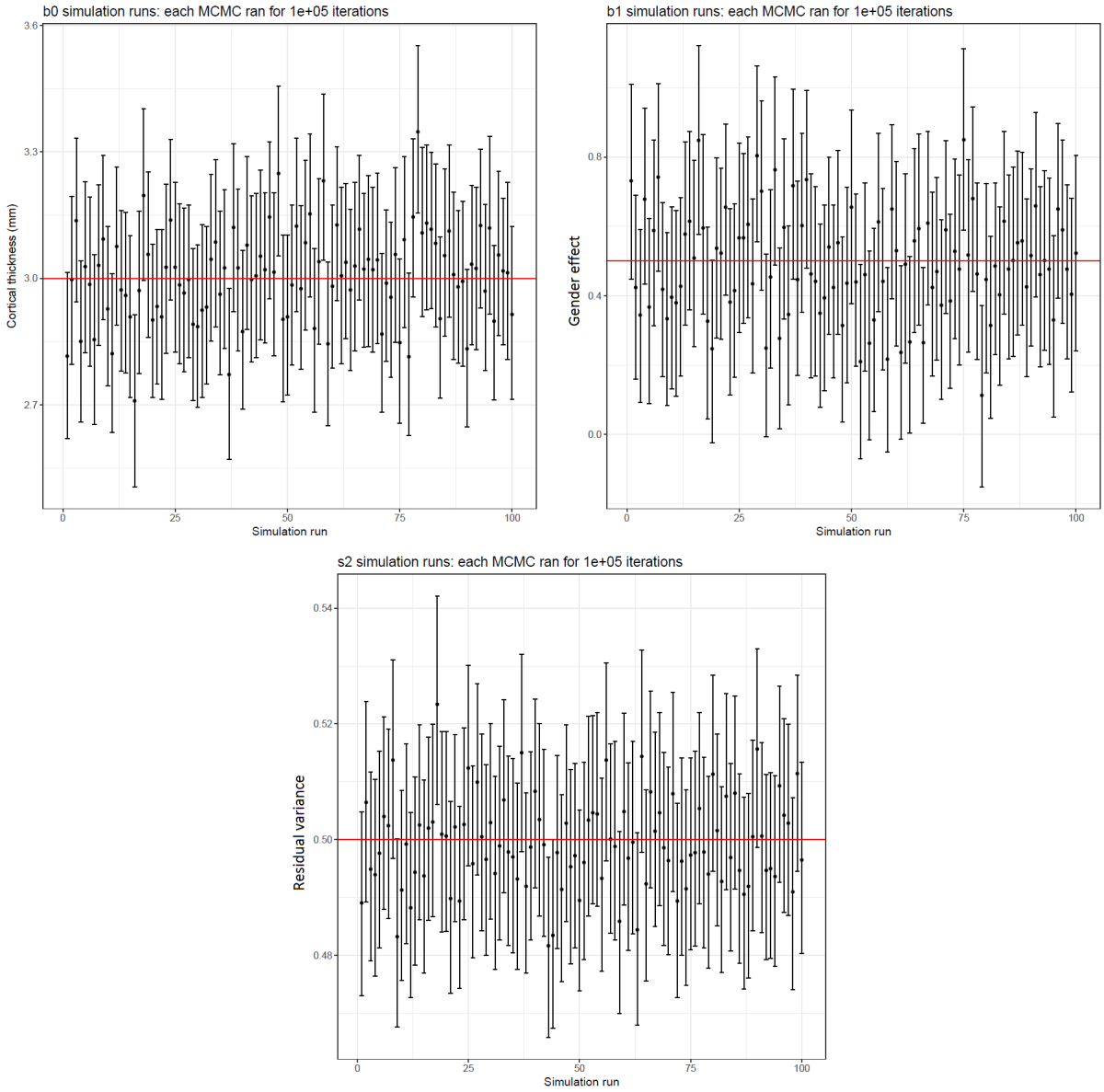

Figure 2: Posterior mean and 95% credible intervals simulation study results for parameters β_0 (top left), β_1 (top right) and σ^2 (bottom) for 100 simulation runs. Each simulation ran for 100,000 MCMC iterations prior to thinning and burn-in. Red line denotes the solution to recover. If the solution lies within the 95% credible interval, then the solution is considered to be recovered.

Figure 4 shows the probability of a connection (p^i_{mn}), between regions m and n over the simulated covariate, standardised age range ($Age_i \in U(-2, 2)$) estimated by the dynamic wombling model, for a single simulated data set. We intentionally generated data which had spatial covariance dynamics over the covariate (via matrices γ^0 and γ^1) in order to assess the models ability to estimate such change and its associated connectivity uncertainty.

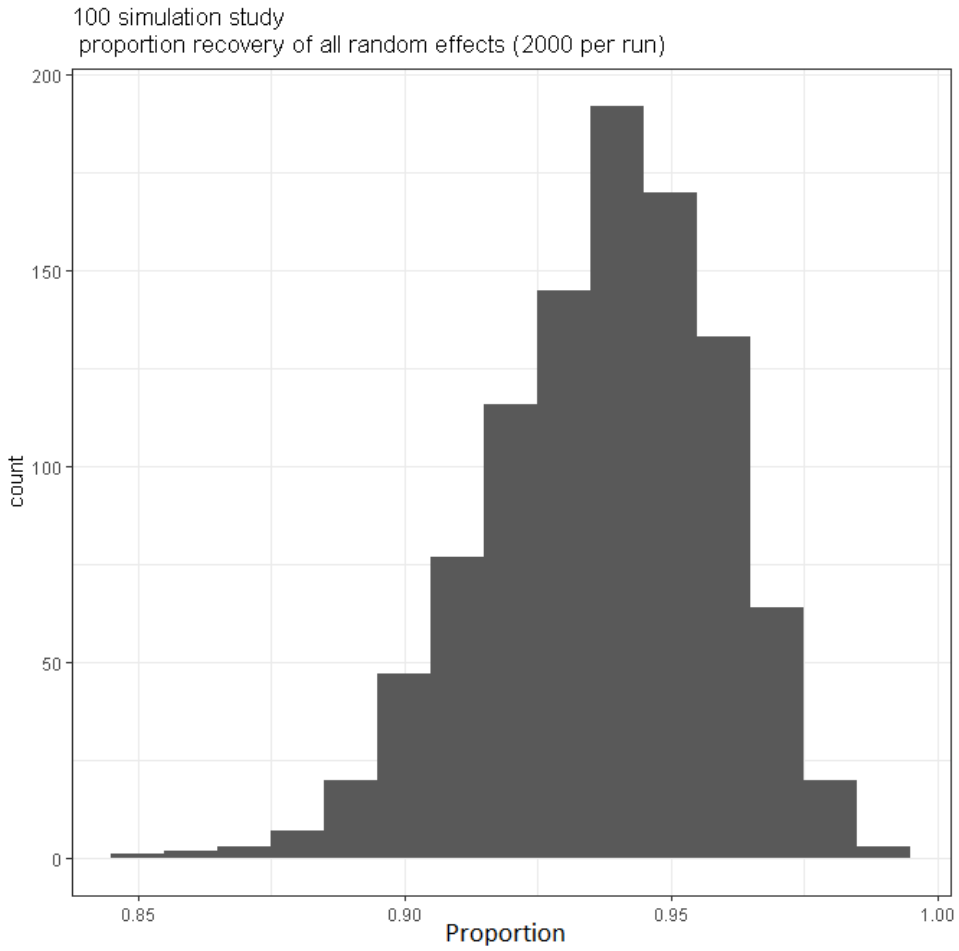

Figure 3: Histogram of the recovered proportion of random effects for the simulation study. The solution was found to be within the 95% credible interval approximately 95% of the time.

S.4 Further simulation analysis: different values for σ^2 and σ_s^2

The simulation study in the manuscript was performed on $\sigma^2 = 0.5$ and $\sigma_s^2 = 1$ with prior distributions $IG(1, 1)$ and $IG(1, 0.5)$ respectively. Here we repeated the analysis with different σ^2 and σ_s^2 values to assess recovery on γ^1, γ^0 and $\boldsymbol{\beta}$. As discussed in the manuscript, a further simulation study on $\sigma^2 = 0.1$ and $\sigma_s^2 = 0.5$ was performed with priors $IG(1, 1)$ and $IG(7, 1)$ respectively. The same simulated values for γ^0, γ^1 and $\boldsymbol{\beta}$ as mentioned in the manuscript were used.

Figure 5 shows the posterior densities for β_0, β_1 and σ^2 for MCMC = 50,000 after discarding the first 10,000 and retaining every 20^{th} iteration. Note, all chains, including those for γ^1 and γ^0, were initialised away from the solution. The solution for each parameter is shown by the red line. As described in the manuscript, parameter σ_s^2 showed systematic bias and did not recover the solution ($\sigma_s^2 = 0.5$).

Figure 6 shows the posterior means and solution to recover for γ^1 and γ^0 parameters. The 95% credible interval for the upper-diagonal (excluding the diagonal elements) on both matrices was evaluated and, with the exception of two elements in γ^1, all credible intervals included the solution to recover. Thus, these results show adequate recovery of parameters for the dynamic wombling model on simulated data with different variance terms

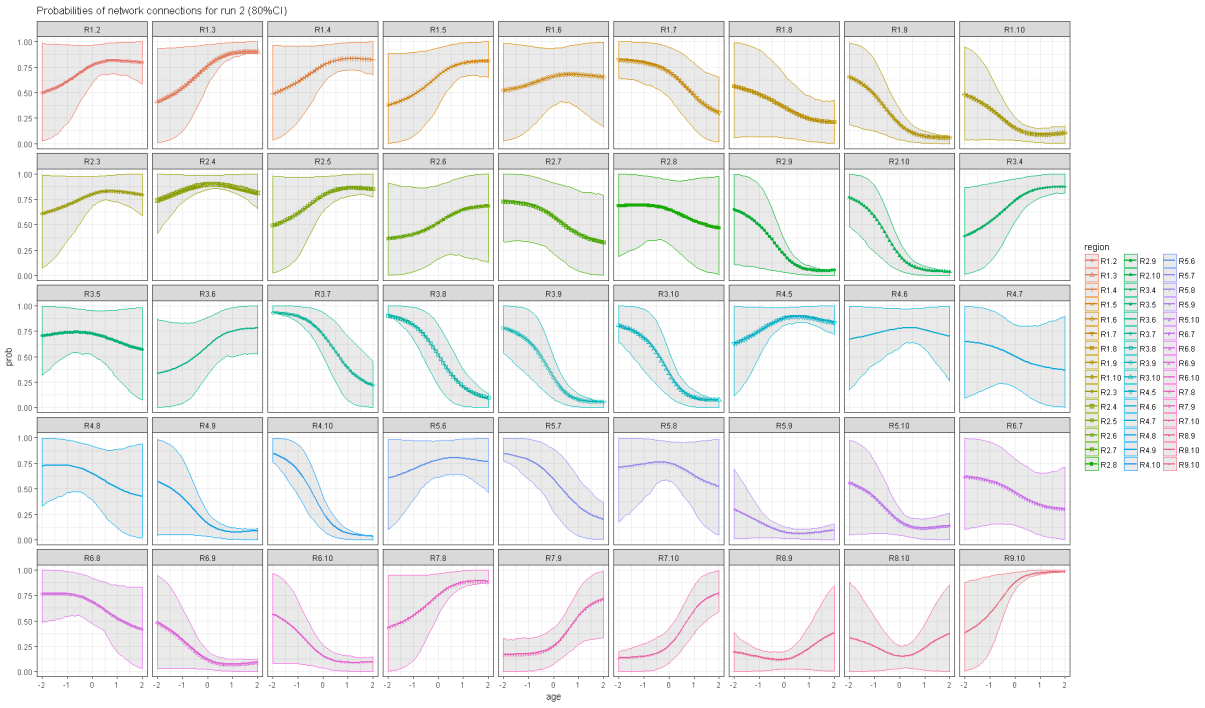

Figure 4: Probability of connections over age range for a single simulation run of the dynamic wombling model. The median of the posterior predictive distribution for each link over age is plotted in conjunction with the 80% credible intervals. The varying credible interval widths reflect models ability to detect the presence or absence of a connection with respect to age. As the data was randomly generated, we expect our estimates to reflect this variation. The simulation study combined the results from 100 independent runs to rigorously assess the performance of the algorithm.

to those in the manuscript. For further diagnostic details or additional simulation results with different values for $\gamma^0, \gamma^1, \sigma^2, \sigma_s^2$ and $\boldsymbol{\beta}$, contact the author.

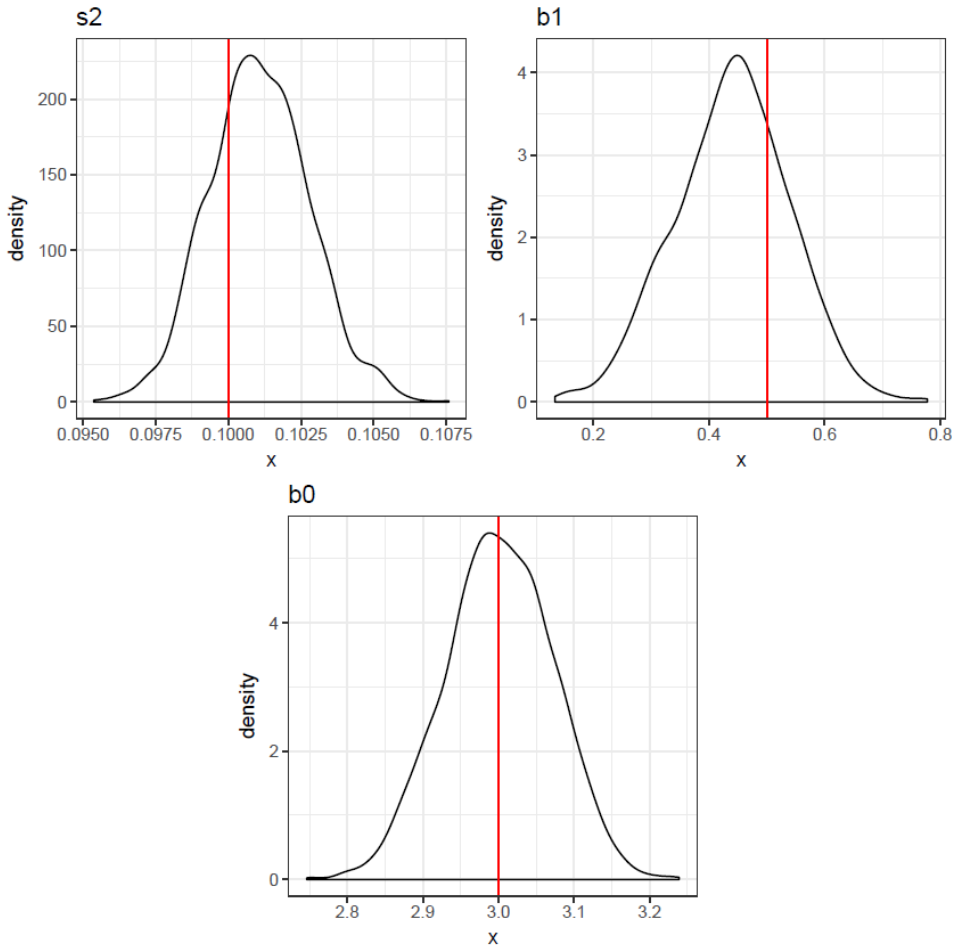

Figure 5: Posterior densities for σ^2 (top left), β_1 (top right) and β_0 (bottom). The solution was within the 95% credible intervals for each density (not included in results).

.

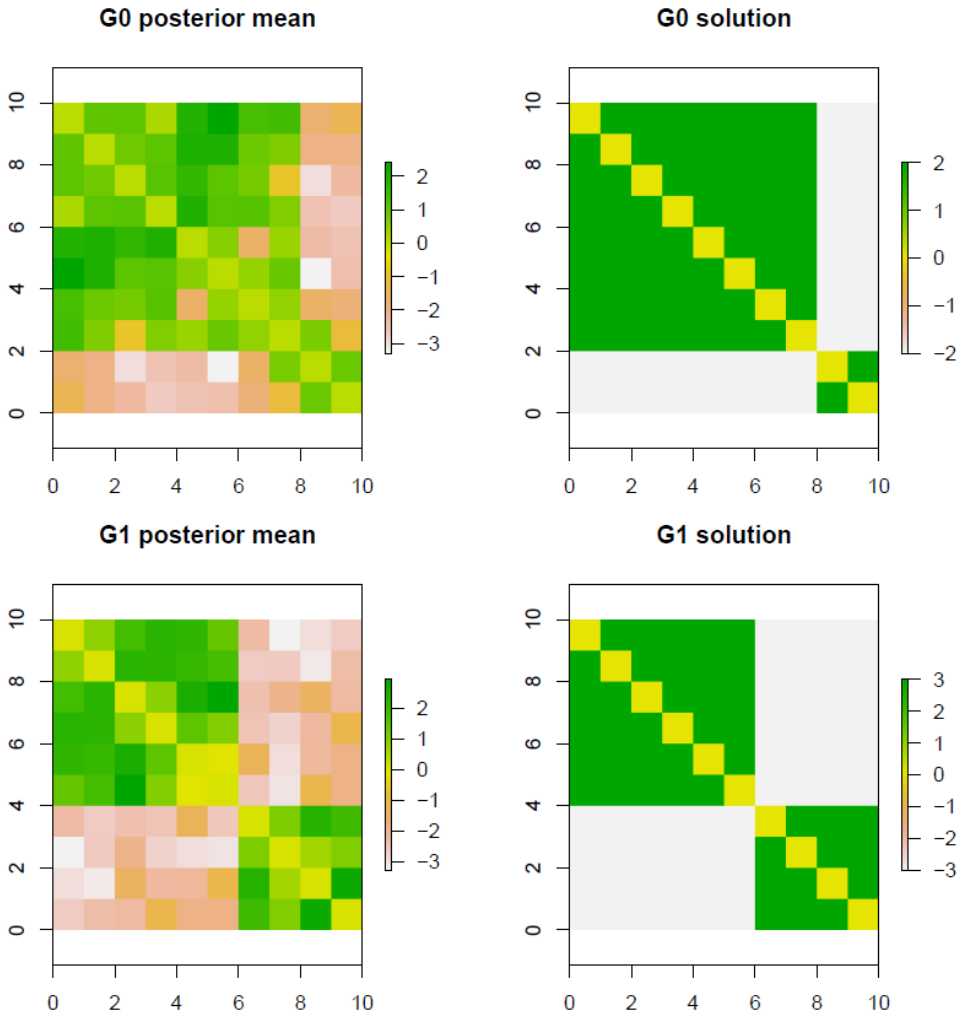

Figure 6: Posterior mean and solution to recover for γ^0 (top) and γ^1 (bottom).

S.5 Posterior diagnostic checks for dynamic wombling models on ADNI data set

Goodness-of-fit for the dynamic wombling model was assessed via posterior predictive plots, shown in Figure 7. Both figures show the model fitted the data well in the HC and AD models, as 97% of the all the response values were within the 95% credible intervals of the posterior predictive distributions. The plots in Figure 7 show no apparent systematic departures from the mean or bias in the model predictions.

Table 2 shows the Gelman-Rubin diagnostic upper 95% confidence interval for $\boldsymbol{\beta}, \sigma^2$ and σ_s^2 parameters for each diagnosis group. Contact the author for trace, autocorrelation and density plots for all parameters, including γ^0 and γ^1.

Table 2: Gelman-Rubin diagnostic upper confidence limit values for each group in ADNI study. As the combinations of the four chains for each group had values close to one, we are confident the MCMC algorithm for both diagnosis groups has reached convergence.

Gelman-Rubin diagnostic													
	β_0	β_1	β_2	β_3	β_4	β_5	β_6	β_7	β_8	β_9	β_{10}	σ^2	σ_s^2
HC	1.00	1.00	1.00	1.00	1.00	1.00	1.00	1.00	1.00	1.00	1.02	1.00	1.00
AD	1.00	1.00	1.00	1.00	1.00	1.00	1.00	1.00	1.00	1.00	1.01	0.99	1.01

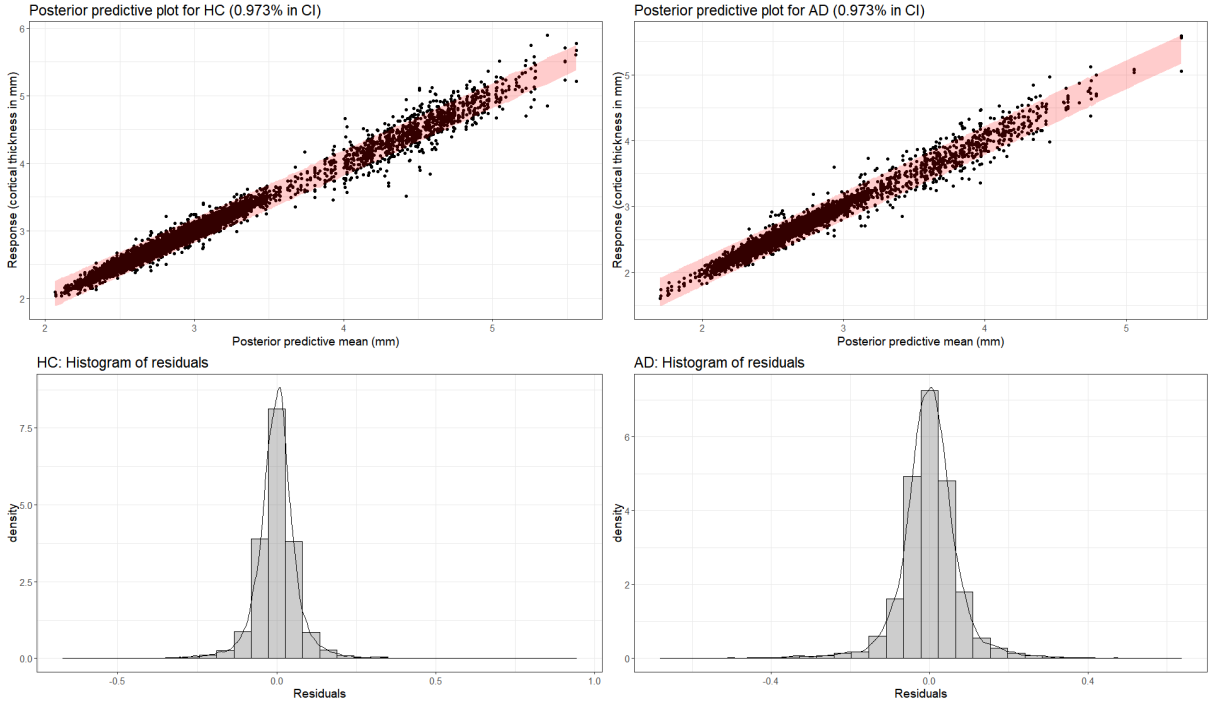

Figure 7: Posterior predictive plot for HC (top left) and AD (top right) diagnosis groups. Red band denotes 95% posterior predictive credible intervals. Histogram of residuals for HC (bottom left) and AD (bottom right).

S.6 Cross validation on dynamic wombling

As the dynamic wombling model consists of a large number of parameters, we performed two approaches of the leave-one-out cross validation (LOOCV) on HC and AD groups to assess for overfitting [6]. Refer to the manuscript for full description of the of cross validation method performed.

LOOCV performance for the first repeated measure on individuals with three or more time points is shown in Figure 8. This plot shows the models had desired predictive performance, despite the slight under-predictive bias. As the scatter plots follow a linear trend ($y = x$), majority of the predictive values lie just under the red line, suggesting they were slightly under-predicted in value. The residuals have an approximate Gaussian distribution suggesting that despite the histogram being symmetric, it is slightly shifted to the left reflecting the slight under-predicted performance. MSE values were 0.029 and 0.033 for HC and AD groups respectively.

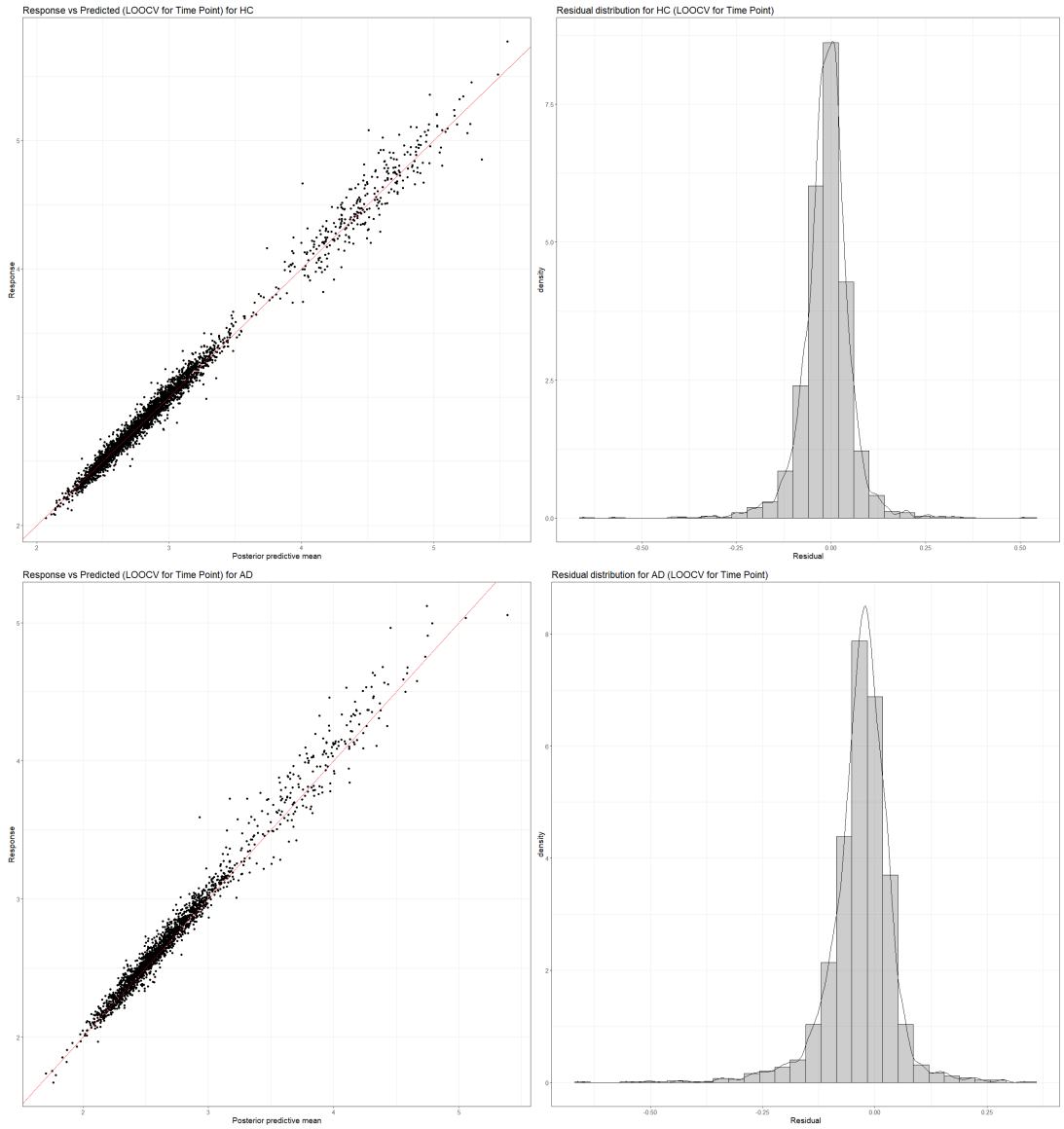

Figure 8: LOOCV for last repeated measure of individuals. Top: response versus predicted scatter plots, red line denotes $y = x$ for HC (left) and AD (right) groups. Bottom: Residual distributions for HC (left) and AD (right) groups.

LOOCV regarding the predictive performance of new individuals and their respective replicates is shown in Figure 9, and was found to be less desirable. These models predicted the means of the ROIs for all individuals and show an unbiased linear trend on the $y = x$ line. HC and AD groups had low MSE values of 0.045 and 0.062 respectively and the residuals had an approximate Gaussian distribution.

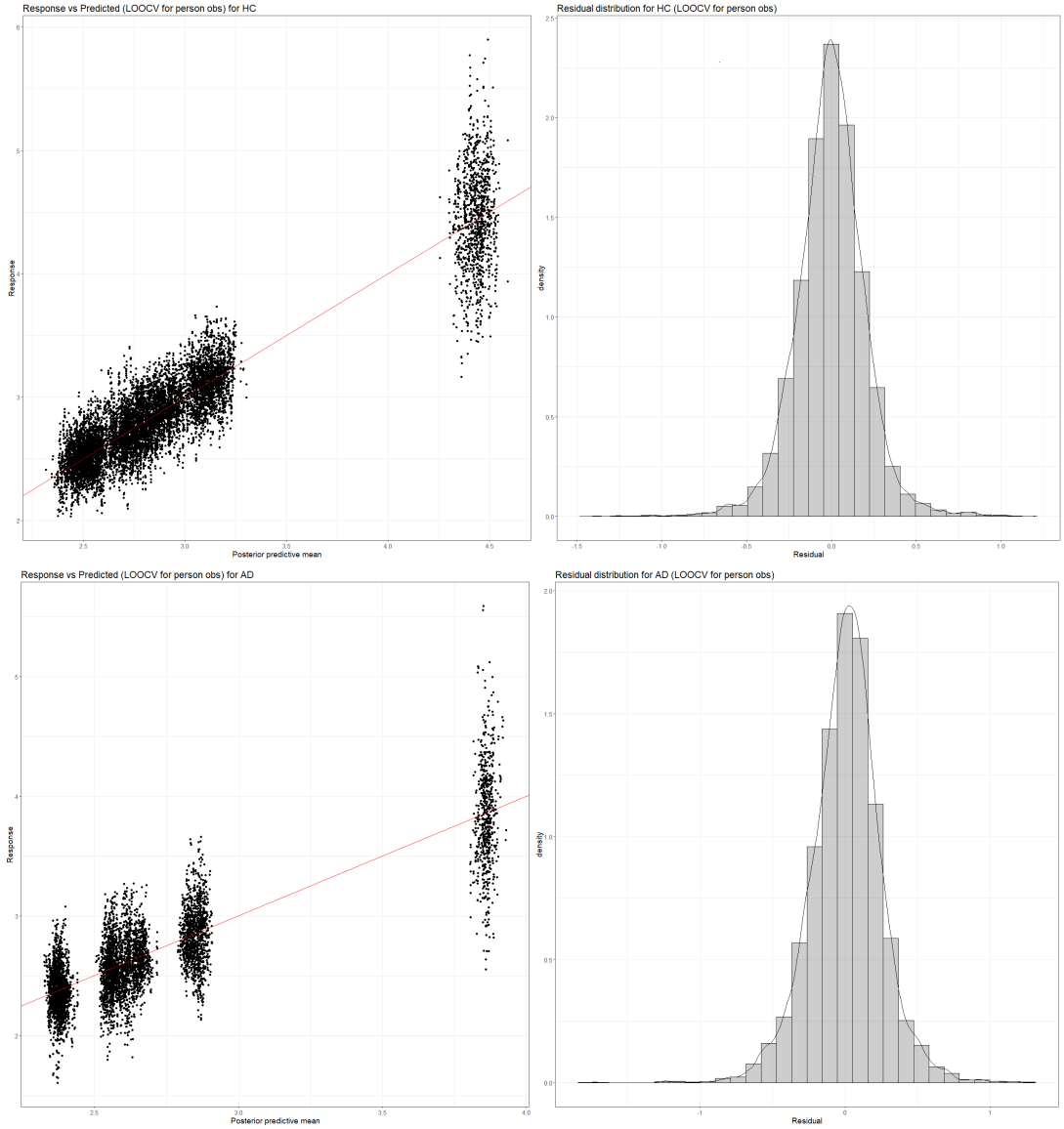

Figure 9: LOOCV for prediction of repeated measures on new individual. Top: response versus predicted scatter plots, red line denotes $y = x$ for HC (left) and AD (right) groups. Bottom: Residual distributions for HC (left) and AD (right) groups.

S.7 Posterior γ_1 and γ_2 estimates

Below are the posterior estimates for γ^0 and γ^1 for HC and AD groups.

	γ^0			γ^1		
$\gamma_{j,k}$	Posterior mean	Low CI	High CI	Posterior mean	Low CI	High CI
$\gamma_{1,2}$	-3.626	-6.24	-1.797	0.065	-4.431	4.566
$\gamma_{1,3}$	2.941	1.001	5.598	-0.033	-4.440	4.279
$\gamma_{1,4}$	4.033	2.111	6.597	-0.051	-4.627	4.371
$\gamma_{1,5}$	0.087	-2.411	1.780	-0.134	-4.499	4.050
$\gamma_{1,6}$	-1.915	-5.063	0.117	0.048	-4.184	4.295
$\gamma_{1,7}$	-0.474	-3.336	1.350	0.108	-4.175	4.468
$\gamma_{1,8}$	-2.160	-5.251	-0.159	-0.005	-4.399	4.371
$\gamma_{1,9}$	-1.578	-4.705	0.275	0.012	-4.333	4.468
$\gamma_{1,10}$	1.342	-0.100	2.999	0.156	-4.145	4.431
$\gamma_{2,3}$	-3.518	-6.140	-1.793	-0.098	-4.431	4.256
$\gamma_{2,4}$	-3.870	-6.477	-2.090	-0.035	-4.281	4.214
$\gamma_{2,5}$	-3.306	-5.912	-1.592	-0.103	-4.513	4.298
$\gamma_{2,6}$	-3.665	-6.335	-1.895	0.137	-4.272	4.641
$\gamma_{2,7}$	-3.622	-6.280	-1.817	0.008	-4.333	4.408
$\gamma_{2,8}$	-2.639	-5.334	-1.034	0.122	-4.249	4.348
$\gamma_{2,9}$	-1.364	-2.969	-0.418	0.309	-3.986	4.706
$\gamma_{2,10}$	-3.278	-5.914	-1.520	0.085	-4.159	4.325
$\gamma_{3,4}$	0.910	-0.540	-2.725	-0.802	-5.195	3.488
$\gamma_{3,5}$	3.554	6.309	-1.562	0.001	-4.290	4.467
$\gamma_{3,6}$	-2.883	-5.722	-0.904	0.001	-4.288	4.358
$\gamma_{3,7}$	-3.121	-6.061	-1.045	-0.095	-4.423	4.397
$\gamma_{3,8}$	-2.943	-5.704	-1.011	-0.118	4.440	4.307
$\gamma_{3,9}$	-0.022	-1.627	1.139	-0.496	-5.048	3.536
$\gamma_{3,10}$	-1.877	-4.923	0.000	-0.056	-4.401	4.334
$\gamma_{4,5}$	-1.792	-4.733	0.153	-0.075	-4.303	4.155
$\gamma_{4,6}$	-2.831	-5.773	-0.702	-0.246	-4.496	3.948
$\gamma_{4,7}$	1.855	0.041	4.357	-0.094	-4.376	4.140
$\gamma_{4,8}$	-2.134	-5.207	-0.250	0.002	-4.398	4.266
$\gamma_{4,9}$	-1.633	-4.439	-0.097	-0.200	-4.352	4.140
$\gamma_{4,10}$	-2.580	-5.483	-0.517	0.112	-4.382	4.690
$\gamma_{5,6}$	-3.002	-5.821	-0.941	0.039	-4.347	4.375
$\gamma_{5,7}$	0.927	-0.950	2.957	0.050	-4.353	4.423
$\gamma_{5,8}$	-0.417	-2.964	1.166	0.291	-4.071	4.797
$\gamma_{5,9}$	-0.809	-3.408	0.792	0.190	-4.189	4.403
$\gamma_{5,10}$	2.019	0.346	4.207	0.003	-4.425	4.350
$\gamma_{6,7}$	4.200	2.395	6.776	-0.049	-4.333	4.243
$\gamma_{6,8}$	0.697	-0.655	2.276	0.226	-4.402	4.762
$\gamma_{6,9}$	-1.573	-4.601	0.178	-0.064	-4.210	4.248
$\gamma_{6,10}$	0.983	-0.508	2.694	0.256	-4.212	4.737
$\gamma_{7,8}$	4.219	2.409	6.741	-0.010	-4.391	4.303
$\gamma_{7,9}$	-2.152	-5.256	0.221	0.046	-4.205	4.414
$\gamma_{7,10}$	-1.651	-4.751	0.520	0.199	-4.208	4.514
$\gamma_{8,9}$	-0.932	-3.687	0.574	0.351	-3.966	4.630
$\gamma_{8,10}$	-2.696	-5.640	0.604	0.231	-4.207	4.641
$\gamma_{9,10}$	-0.313	-2.635	1.296	0.144	-4.223	4.256

Table 3: Posterior estimates for γ^0 and γ^1 for HC group.

	γ^0			γ^1		
$\gamma_{j,k}$	Posterior mean	Low CI	High CI	Posterior mean	Low CI	High CI
$\gamma_{1,2}$	-3.55	-6.227	-1.626	0.344	-3.73	4.458
$\gamma_{1,3}$	3.091	0.875	5.98	-0.06	-4.251	4.135
$\gamma_{1,4}$	4.023	2.11	6.611	-0.432	-4.623	3.705
$\gamma_{1,5}$	1.011	-1.361	3.759	0.516	-3.679	4.702
$\gamma_{1,6}$	-0.958	-4.493	1.923	-0.115	-4.376	4.284
$\gamma_{1,7}$	-2.033	-5.266	0.326	-0.104	-4.431	4.331
$\gamma_{1,8}$	-3.023	-5.894	-0.889	0.306	-3.904	4.503
$\gamma_{1,9}$	-1.542	-5.003	1.112	0.286	-3.840	4.706
$\gamma_{1,10}$	0.642	-2.188	3.165	1.181	-2.684	5.314
$\gamma_{2,3}$	-2.934	-5.724	-1.183	-0.118	-4.055	4.066
$\gamma_{2,4}$	-3.852	-6.524	-1.981	0.482	-3.573	4.678
$\gamma_{2,5}$	-2.770	-5.572	-1.033	-0.298	-4.121	3.877
$\gamma_{2,6}$	-2.887	-5.725	-1.034	0.258	-3.739	4.317
$\gamma_{2,7}$	-3.204	-6.027	-1.305	0.329	-3.850	4.532
$\gamma_{2,8}$	-1.776	-4.207	-0.463	-0.520	-4.573	3.627
$\gamma_{2,9}$	-3.118	-5.890	-1.267	0.491	-3.478	4.619
$\gamma_{2,10}$	-2.896	-5.685	-1.108	-0.181	-4.233	3.983
$\gamma_{3,4}$	0.734	-1.185	3.215	-0.099	-4.437	3.992
$\gamma_{3,5}$	-2.481	-5.599	-0.330	0.062	-4.491	4.386
$\gamma_{3,6}$	-2.695	-5.666	-0.565	-0.077	-4.412	4.247
$\gamma_{3,7}$	-3.211	-6.110	-1.139	0.028	-4.320	4.387
$\gamma_{3,8}$	-2.833	-5.664	-0.806	0.217	-4.102	4.493
$\gamma_{3,9}$	-1.687	-4.834	0.394	-0.438	-4.732	4.009
$\gamma_{3,10}$	-0.151	-2.824	1.687	-1.021	-5.145	3.384
$\gamma_{4,5}$	-1.497	-4.742	0.789	0.300	-4.000	4.398
$\gamma_{4,6}$	-1.895	-5.200	0.651	0.065	-4.295	4.288
$\gamma_{4,7}$	0.273	-2.482	2.608	-0.268	-4.451	3.671
$\gamma_{4,8}$	-2.36	-5.428	0.005	0.404	-3.556	4.343
$\gamma_{4,9}$	0.980	-1.187	3.464	-0.777	-4.870	3.396
$\gamma_{4,10}$	-1.940	-5.181	0.360	0.653	-3.702	4.923
$\gamma_{5,6}$	-0.845	-4.104	1.492	-0.014	-4.432	4.501
$\gamma_{5,7}$	-2.558	-5.546	-0.394	0.086	-3.943	4.297
$\gamma_{5,8}$	-3.067	-5.949	-0.957	0.155	-3.788	4.276
$\gamma_{5,9}$	0.161	-2.453	2.369	0.289	-3.699	4.310
$\gamma_{5,10}$	3.783	1.786	6.443	-0.328	-4.581	3.822
$\gamma_{6,7}$	3.986	2.017	6.602	-0.401	-4.632	3.763
$\gamma_{6,8}$	1.315	-1.092	4.555	-0.228	-4.541	4.071
$\gamma_{6,9}$	-0.735	-4.116	1.556	0.918	-3.439	4.931
$\gamma_{6,10}$	0.481	-2.024	2.610	1.111	-2.930	5.077
$\gamma_{7,8}$	4.297	2.413	6.838	-0.316	-4.566	3.968
$\gamma_{7,9}$	-1.488	-4.874	0.846	0.866	-3.382	4.908
$\gamma_{7,10}$	-2.716	-5.959	-0.493	0.270	-4.023	4.509
$\gamma_{8,9}$	-2.340	-5.458	-0.286	0.784	-3.515	5.18
$\gamma_{8,10}$	-2.911	-5.458	-2.286	0.042	-4.219	4.393
$\gamma_{9,10}$	-0.368	-3.779	2.290	0.256	-4.047	4.477

Table 4: Posterior estimates for γ^0 and γ^1 for AD group.

S.8 Posterior inference $P(\gamma_{HC} > \gamma_{AD})$

A described in Section 4.1 of the manuscript, below are the full list of $P(\gamma_{HC} > \gamma_{AD})$ probabilities to compare γ^0 and γ^1 estimates between HC and AD groups.

$\gamma_{j,k}$	γ_1 comparisons between HC and AD $P\left(\gamma^0_{HC} > \gamma^0_{AD}\right)$	γ_1 comparisons between HC and AD $P\left(\gamma^1_{HC} > \gamma^1_{AD}\right)$
$\gamma_{1,2}$	0.457	0.500
$\gamma_{1,3}$	0.523	0.455
$\gamma_{1,4}$	0.552	0.468
$\gamma_{1,5}$	0.361	0.204
$\gamma_{1,6}$	0.546	0.403
$\gamma_{1,7}$	0.529	0.811
$\gamma_{1,8}$	0.463	0.750
$\gamma_{1,9}$	0.477	0.516
$\gamma_{1,10}$	0.446	0.680
$\gamma_{2,3}$	0.506	0.347
$\gamma_{2,4}$	0.419	0.510
$\gamma_{2,5}$	0.515	0.354
$\gamma_{2,6}$	0.477	0.319
$\gamma_{2,7}$	0.508	0.347
$\gamma_{2,8}$	0.590	0.272
$\gamma_{2,9}$	0.502	0.939
$\gamma_{2,10}$	0.559	0.369
$\gamma_{3,4}$	0.341	0.506
$\gamma_{3,5}$	0.452	0.259
$\gamma_{3,6}$	0.486	0.444
$\gamma_{3,7}$	0.504	0.509
$\gamma_{3,8}$	0.477	0.474
$\gamma_{3,9}$	0.461	0.886
$\gamma_{3,10}$	0.652	0.157
$\gamma_{4,5}$	0.406	0.483
$\gamma_{4,6}$	0.414	0.322
$\gamma_{4,7}$	0.511	0.803
$\gamma_{4,8}$	0.465	0.516
$\gamma_{4,9}$	0.528	0.037
$\gamma_{4,10}$	0.437	0.335
$\gamma_{5,6}$	0.549	0.066
$\gamma_{5,7}$	0.499	0.994
$\gamma_{5,8}$	0.500	0.957
$\gamma_{5,9}$	0.450	0.317
$\gamma_{5,10}$	0.503	0.142
$\gamma_{6,7}$	0.571	0.560
$\gamma_{6,8}$	0.585	0.261
$\gamma_{6,9}$	0.290	0.223
$\gamma_{6,10}$	0.361	0.663
$\gamma_{7,8}$	0.545	0.494
$\gamma_{7,9}$	0.373	0.400
$\gamma_{7,10}$	0.483	0.735
$\gamma_{8,9}$	0.437	0.791
$\gamma_{8,10}$	0.536	0.541
$\gamma_{9,10}$	0.471	0.458

Table 5: Posterior estimates for γ^0 and γ^1 for AD group.

S.9 participant ROI estimates

Refer to the manuscript for a description of cortical thickness estimates estimates for the 10 ROIs used in this work as well as the participant estimates. Figure 10 shows the caterpillar plots for all participants in this analyses.

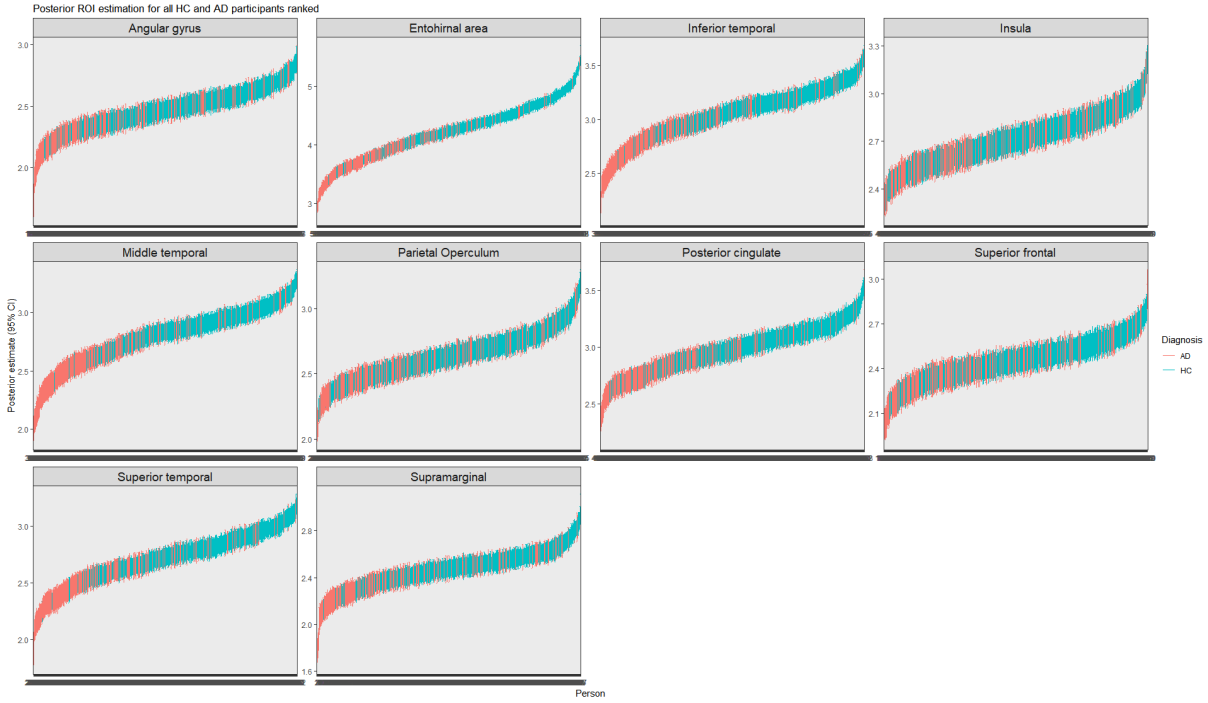

Figure 10: Caterpillar plots with 95% credible intervals for each participant's cortical thickness estimate at baseline age, for healthy control (blue) and Alzheimer's disease (red) groups for all 10 ROIs. Participants are ranked according to posterior mean estimates of cortical thickness for each ROI.

S.10 Joint HC and AD analyses

Results from joint HC and AD analyses in the inverse-logit term in Expression (5) of the manuscript, as described in Section 4.2 are presented here. As the extension was in relation to the terms in the inverse-logit, the changes in the full conditionals for $p(w^i_{mn}|.)$ and $p(\boldsymbol{\gamma}_{mn}|.)$ were straightforward to implement and were omitted here. Below we present the full conditional distribution for $p(\delta_0|.)$, and in a similar manner, it follows, that the full conditionals for $p(\delta_1|.)$ can also be derived. Recall that the prior for δ_0 is $p(\delta_0) \sim N(\mu_0, \sigma_0^2)$, the full conditionals for $p(\delta_0|.)$ is

$$\log[p(\delta_0|\delta_1, \boldsymbol{\gamma}, W, CS)] \propto \sum_{i=1}^{I}\sum_{m=1}^{K}\sum_{n>m}^{K} w^i_{mn}(\alpha_{imn}) - \log(1+\exp(\alpha_{imn})) - \frac{1}{2\sigma_0^2}(\delta_0 - \mu_0)^2 \tag{6}$$

where $\alpha_{imn} = \gamma^0_{mn} + \delta_0 \mathbb{I}_{AD,i} + \gamma^1_{mn} CS_i + \delta_1 \mathbb{I}_{AD,i} CS_i$. The random walk variance of the MH algorithm used to draw posterior samples for δ_0 and δ_1 were chosen, such that the acceptance rates were 42% and 67%, respectively. Two 50,000 MCMC chains were drawn for this model with different starting values, and convergence for δ_0 and δ_1, as well as all other parameters were assessed in a similar manner as described in the manuscript. Contact the author for posterior estimates for γ^0 and γ^1, full posterior model convergence diagnostics and posterior predictive plots.

Figure 11: Median posterior probability trajectories over average annual relative change of cognitive score for HC (blue) and AD (red) connections among 10 ROI with 80% credible intervals. These trajectories were derived from extended Model (5). See Table 1 in manuscript for ROI names and enumeration.

Table 6: Extended dynamic wombling model ROI posterior cortical thickness means for 10 ROIs with 95% credible intervals in parenthesis for joint analyses of Healthy Control (HC) and Alzheimer's disease (AD) groups. Refer to Table 1 in manuscript for ROI names.

ROI	HC & AD combined estimates
1	2.451 (2.433, 2.469)
2	4.233 (4.198, 4.269)
3	2.436 (2.417, 2.455)
4	2.449 (2.431, 2.467)
5	2.621 (2.602, 2.640)
6	2.714 (2.696, 2.732)
7	2.800 (2.782, 2.819)
8	3.051 (3.032, 3.070)
9	2.969 (2.951, 2.988)
10	2.700 (2.681, 2.718)
Baseline age (β_{11})	-0.043 (-0.06, -0.029)

References

[1] M. I. Cespedes, J. McGree, C. C. Drovandi, K. Mengersen, J. D. Doecke, and J. Fripp. A Bayesian hierarchical approach to jointly model structural biomarkers and covariance networks, November 2017. QUT ePrints: 112807: https://eprints.qut.edu.au/112807.

[2] S. Chib and E. Greenberg. Understanding the Metropolis-Hastings algorithm. *The American Statistician*, 49(4):327–335, 1995.

[3] A. Gelman, J. B. Carlin, H. S. Stern, D. B. Dunson, A. Vehtari, and D. B. Rubin. *Bayesian data analysis*. CRC press, 2^{nd} edition, 2013. ISBN 9780429113079.

[4] H. Lu, C. S. Reilly, S. Banerjee, and B. P. Carlin. Bayesian areal wombling via adjacency modeling. *Environmental and Ecological Statistics*, 14(4):433–452, 2007.

[5] N. Metropolis, A. W. Rosenbluth, M. N. Rosenbluth, A. H. Teller, and E. Teller. Equation of state calculations by fast computing machines. *The Journal of Chemical Physics*, 21(6):1087–1092, 1953.

[6] W. Wang and A. Gelman. Difficulty of selecting among multilevel models using predictive accuracy. *Statistics at its Interface*, 7(1):1–88, 2014.